Water Supply

Water Supply Vol 22 No 4, 3769 doi: 10.2166/ws.2022.022

Approaches for estimating mixing time in a water storage tank

Jie Zhang *
Research & Development Group, Carollo Engineers, Inc., 4600 E Washington St Suite 500, Phoenix, AZ 85034, USA
E-mail: jzhang@carollo.com

JZ, 0000-0002-0906-0099

ABSTRACT

The mixing performance of a water storage tank is important to ensure good drinking water quality in a distribution system. A tracer study is a commonly used approach for mixing performance evaluation but has limitations, such as limited sampling points and inability to be applied to the full scale at design stage. In practice, mixing time is usually estimated by the tracer curve measured by a probe sensor in a physical tracer study. However, the probe tracer concentration curve can be affected by many factors in the tracer release approach (e.g., instantaneous pouring or quill injecting), such as pouring volume, vertical penetration, and injecting time, making the estimated mixing time inaccurate. Coefficient of variation (CoV) decay curve is an alternative for determining mixing time. In this study, computational fluid dynamics (CFD) models were developed to study mixing in a cylindrical water tank. Mixing times were estimated from both probe tracer curve and CoV decay curve. Results show that the mixing time estimated from a probe tracer curve only represents local mixing, while that estimated from a CoV decay curve is a more appropriate index for global mixing, suggesting that the CoV decay curve should be used for mixing performance analysis in a water tank.

Key words: computational fluid dynamics, mixing, tracer study, water storage tank

HIGHLIGHTS

- Compared two approaches for estimating mixing time in water storage tanks.
- Probe tracer curve predicts inaccurate mixing time and highly depends on tracer release method.
- CoV decay curve predicts accurate mixing time and less dependent on tracer release method.
- CoV decay curve is suggested for both physical and numerical mixing analysis of water tank.

INTRODUCTION

The water storage tank or reservoir is an important part in a drinking water distribution system for equalizing pumping requirements and operating pressures, and emergency water use such as firefighting and pumping outages. Complete and fast mixing in a water storage tank is essential to maintain high water quality in the drinking water distribution system. Therefore, the mixing performance of a water storage tank is usually evaluated at the design stage. However, many factors can affect the completeness and speed of mixing in a water storage tank. These factors include tank configuration, diameter, angle, and location of injection pipe, numbers of inlets and outlets, injection velocity, and water level and so on (Bumrungthaichaichan 2016; Xavier & Janzen 2017). It makes an accurate evaluation of mixing performance a challenge at the design stage. Many empirical models were developed for estimating the mixing time in a storage tank. The most recent are a model developed for a specific tank with two jets horizontally located at one-half and one-third of tank height (Simon & Fonade 1993; Orfaniotis *et al.* 1996) and a model for a series of cylindrical tanks with diameter ranges from 0.61 m to 36 m and height/diameter ratio ranges from 0.2 to 1.0 (Grenville & Tilton 1996, 1997, 2011). Bumrungthaichaichan (2016) well summarized these empirical models in a review paper. The empirical models were useful for a specific application but limited for broader applications. They also cannot apply to some advanced designs with complex nozzle systems. Therefore, a lab or pilot-scale physical test is more reliable to accurately evaluate the mixing performance of a new design compared to these empirical models. The reported physical testing approaches for studying the mixing in a water storage tank are a tracer (or dye) study (Rossman & Grayman 1999; Hurtig 2004; Sautner *et al.* 2007) and a three-dimensional laser-induced fluorescence

(3DLIF) system (e.g., Roberts 2006; Tian & Roberts 2008a, 2008b). The high cost of 3DLIF limits its application, making a tracer study the most used approach to study mixing in water storage tank. However, a physical tracer study still has some limitations: sampling points limited by the number of sensors; cannot be conducted on the full-scale in the design stage; many factors in operation may bring in significant errors to the results of the tracer study (Zhang *et al.* 2019a).

The rapid advancement of computational fluid dynamics (CFD) application in water engineering in recent years provides engineers an option to conduct a tracer study numerically. It can overcome the limitations of a physical tracer study and may push down the cost further (Zhang *et al.* 2019b). Many studies have reported their successful CFD modeling of the mixing in a water storage tank. Although CFD is a powerful tool, it is still in the process of being polished. There are a few challenges that need to be solved in CFD modeling. For example, Marek *et al.* (2007) simulated a laboratory physical tracer experiment conducted in a water mixing tank by Gaikwad (2001) using CFD but found a significant discrepancy between their CFD predicted tracer curve at the probe sensors and the measurements (Marek *et al.* 2007). Although the CFD results by Marek *et al.* (2007) showed an improvement compared to the CFD results from Patwardhan & Gaikwad (2003), the significant discrepancy between CFD and measurement still exists, and the reason was not explained.

To better understand the discrepancy between the CFD prediction and physical measurement of the water storage tank, this work investigated the uncertainty of mixing effect induced by different approaches to how tracer is released at the beginning (i.e., the initial condition) and revealed that the initial condition of tracer study may play a critical role in tracer analysis. Note that this study on the tracer release initial condition was also inspired by the fact that in the physical tracer study of a water storage tank in a water treatment plant, it is common to pour a bulk of tracer solution into the water storage tank through the access hatch on the top of the water storage tank (as shown in Figure 1). The results of this study also demonstrated that the mixing time determined by the probe tracer curve could be inaccurate, and the mixing time estimated by a coefficient of variation (CoV) decay curve is more reliable. These findings of this study improve the understanding of mixing in a water storage tank and provide useful instructions for future physical tracer study.

METHODS

Governing equations and simulation methods

The unsteady Reynolds-averaged Navier-Stokes (URANS) equations were solved for the water flow since the inlet jet has a transient feature and can impact tracer results significantly. The governing equations include the incompressible Reynolds-averaged continuity equation and momentum (Navier-Stokes) equations:

$$\frac{\partial \langle u_i \rangle}{\partial x_i} = 0 \tag{1}$$

$$\frac{\partial \langle u_i \rangle}{\partial t} + \langle u_j \rangle \frac{\partial \langle u_i \rangle}{\partial x_j} = -\frac{1}{\rho}\frac{\partial \langle p \rangle}{\partial x_i} + \nu \frac{\partial^2 \langle u_i \rangle}{\partial x_j^2} - \frac{1}{\rho}\frac{\partial \left\langle u_i' u_j' \right\rangle}{\partial x_j} \tag{2}$$

where a bracket denotes Reynolds or ensemble averaging, $\langle u_i \rangle$ is the averaged velocity, x_i is the position vector, t is time, $\langle p \rangle$ is the averaged pressure, ρ is the constant density, and ν is the constant kinematic viscosity. The Reynolds stress tensor $-\left\langle u_i' u_j' \right\rangle$ (expressed in terms of velocity fluctuation u_i') presents a closure problem because u_i' is not known as the simulation only

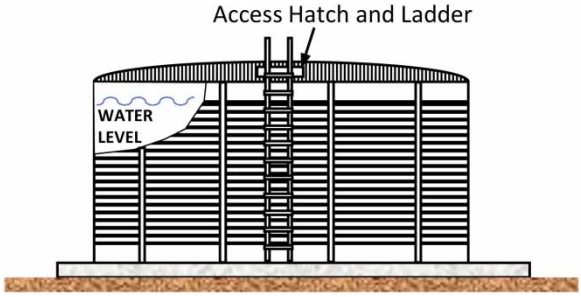

Figure 1 | Schematic of a typical water storage tank in a water treatment plant.

computes the mean flow. Closure of the Reynolds stress is obtained via an eddy viscosity model of the form

$$-\left\langle u_i' u_j' \right\rangle = \mu_t \frac{\partial \langle u_i \rangle}{\partial x_j} \tag{3}$$

where the eddy viscosity is

$$\mu_t = C_\mu \frac{k^2}{\varepsilon} \tag{4}$$

In the latter expression, k is the turbulent kinetic energy and ε is the turbulent kinetic energy dissipation rate. Transport equations for k and ε are specified via the realizable k-ε model equipped with standard wall functions (Wilcox 1994).

Average passive tracer concentration $\langle C \rangle$ is computed from the Reynolds-averaged scalar advection-diffusion equation:

$$\frac{\partial \langle C \rangle}{\partial t} + \langle u_j \rangle \frac{\partial \langle C \rangle}{\partial x_j} = -\frac{\partial \langle u_i' C' \rangle}{\partial x_j} \tag{5}$$

where C' denotes tracer fluctuation and turbulent scalar flux $\langle u_i' C' \rangle$ is closed as

$$-\langle u_i' C' \rangle = D_t \frac{\partial \langle C \rangle}{\partial x_j} \tag{6}$$

The eddy (turbulent) diffusivity is taken as $D_t = \nu_t / Sc_t$ where eddy viscosity ν_t (defined as $\nu_t = \mu_t / \rho$) is computed via the realizable k-ε model and the turbulent Schmidt number, Sc_t, is taken as 0.7 (Launder 1978).

Since the jet mixing in the storage tank includes some unsteady flow features, the momentum and tracer transport equations are solved sequentially at each time step to accurately capture the change of flow field over time.

Experimental setup

The mixing test conducted in the laboratory-scale water storage tank (Patwardhan & Gaikwad 2003) was selected for this study. The diameter and height of the water storage tank were 0.50 m and 0.75 m, respectively. The water level in the tank was kept equal to 0.5 m. The outlet of the tank was 0.0381 m in diameter and was located at 0.05 m from tank bottom. A pump was used to recycle part of the liquid from the tank and return it to the tank with a high velocity through a nozzle. The schematic of the experimental setup is shown in Figure 2. Different angles and diameters of the nozzle were tested in Patwardhan & Gaikwad (2003). But in this study, only the nozzle with diameter 8 mm and a 45-degree injection angle was considered. For the mixing test, according to the record, a certain amount of sodium chloride solution was added as a tracer pulse at the center of the tank at the water surface. However, it is not clear what were: (1) the mass or volume of the initial tracer; (2) the injection velocity; (3) the duration of the pulse. Tracer concentrations at probe sensors 1 and 2 were recorded over time for further analysis.

Numerical settings

Three-dimensional CFD simulations were carried out by commercial software ANSYS Fluent 19.2 (refer to ANSYS Fluent (2016) for more information of this software). The grid used for the simulations is shown in Figure 3. It has about 1 million elements in total, which was determined by a grid independence study with four sets of meshes. A non-slip boundary condition with zero shear stress is imposed at the water surface. A velocity boundary condition is imposed at the inlet with inlet flow velocity held constant at 4.4 m/s. The turbulence quantities at the inlet were specified by the intensity and hydraulic diameter method in ANSYS Fluent. The turbulent intensity was 5% and the hydraulic diameter was 8 mm, which was the diameter of the inlet pipe. The pressure gradient at the outlet is set to zero. Non-slip boundary conditions were imposed at the bottom and side walls. At the outlet and walls, the normal gradients of tracer concentration were set to zero, indicating zero diffusive flux across these boundaries.

To investigate the impact of tracer initial condition on the tracer analysis results, two tracer introducing approaches were considered. The first one is instantaneous pouring. This approach pours a bulk of tracer solution into the system instantaneously (usually from the access hatch of the water storage tank in practice). This approach is easy to operate since it

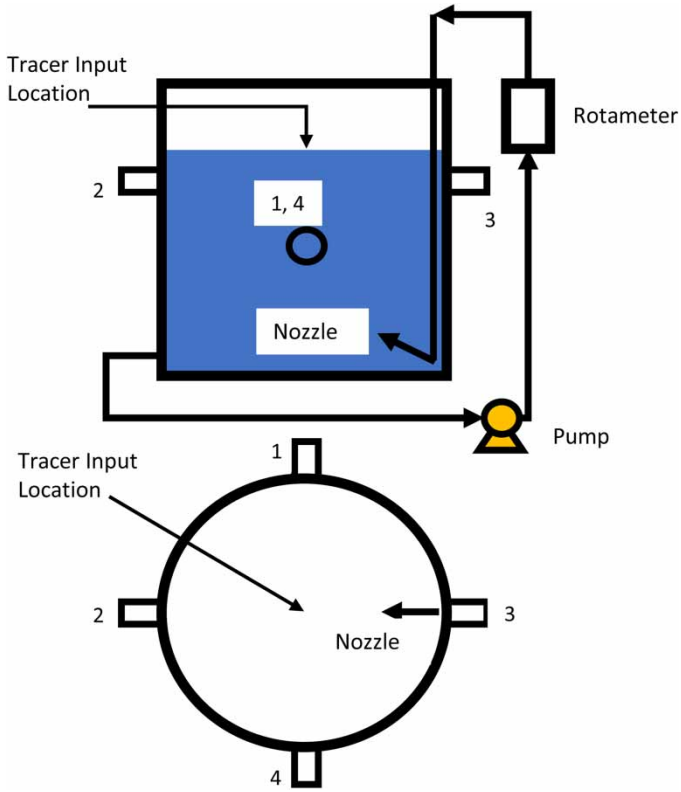

Figure 2 | Schematic of experimental setup for the mixing test in a water storage tank (adapted from Patwardhan & Gaikwad (2003)). Numbers 1 through 4 indicate probe sensors.

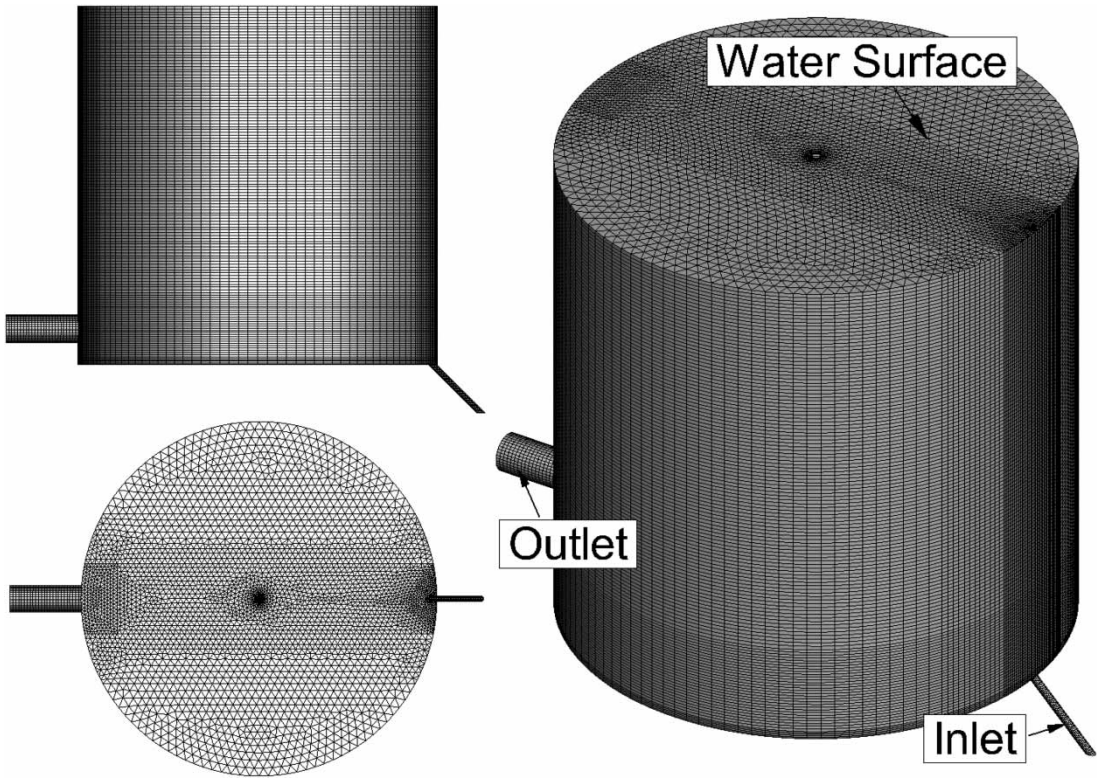

Figure 3 | Geometry and Mesh of the mixing tank CFD model.

does not require tracer injecting equipment, but it brings uncertainties since there are nospecific requirements for the solution volume to be poured and how to pour it. Considering different solution volumes (note that the initial tracer concentration keeps the same) and pouring momentum, ten possible scenarios were simulated using CFD for the first approach. The initial tracer distributions of the ten scenarios are shown in Figure 4. The second approach is quill injecting. This approach injects tracer solution with the same concentration as the instantaneous pouring approach into the system through a quill, which is a tube with a small diameter (i.e., 8 mm), for a short-time period. This study considered 1, 4, and 10 seconds, corresponding to roughly 0.25%, 1%, and 2.5% of the hydraulic retention time (i.e., 444 seconds, defined as the ratio of tank volume divided by influent flow rate) of the mixing tank, for the initial tracer release period, respectively. All the tracer release approaches are summarized in Table 1.

All the simulations were run on a workstation with 4-core CPU and 64 GB memory. It took around 20 hours on the 4 cores to run one scenario listed in Table 1.

Approaches to quantify mixing level

To quantify the mixing level in the storage tank, the concept of mixing time was used in this study. A shorter mixing time indicates a better mixing. Two approaches were considered for the prediction of mixing time.

The first approach is based on Residence Time Distribution (RTD), which is generated by monitoring the tracer concentration at target locations in the tracer study. In this approach, the mixing time was considered as the time it takes to reach 95% of the completely mixed concentration (Patwardhan & Gaikwad 2003).

The second approach estimates the mixing time from the decay curve of tracer CoV. CoV is calculated by (standard deviation of tracer concentration)/(mean tracer concentration). Therefore, a small CoV indicates a well-mixed status. The CoV is large when the tracer pulse is released at the beginning. It will decay as time progresses. When CoV decays to 0.1, it is considered to be well mixed (Roberts 2006; Tian & Roberts 2008a). The time it takes to the well-mixed status is considered to be the mixing time in this approach.

RESULTS AND DISCUSSION

Flow field and tracer distribution

All the tracer simulations were conducted after the flow had been fully developed. As shown in Figure 5, the fully developed flow is characterized by a high-speed jet and a recirculation on the two sides. The high-speed jet shoots diagonally from the

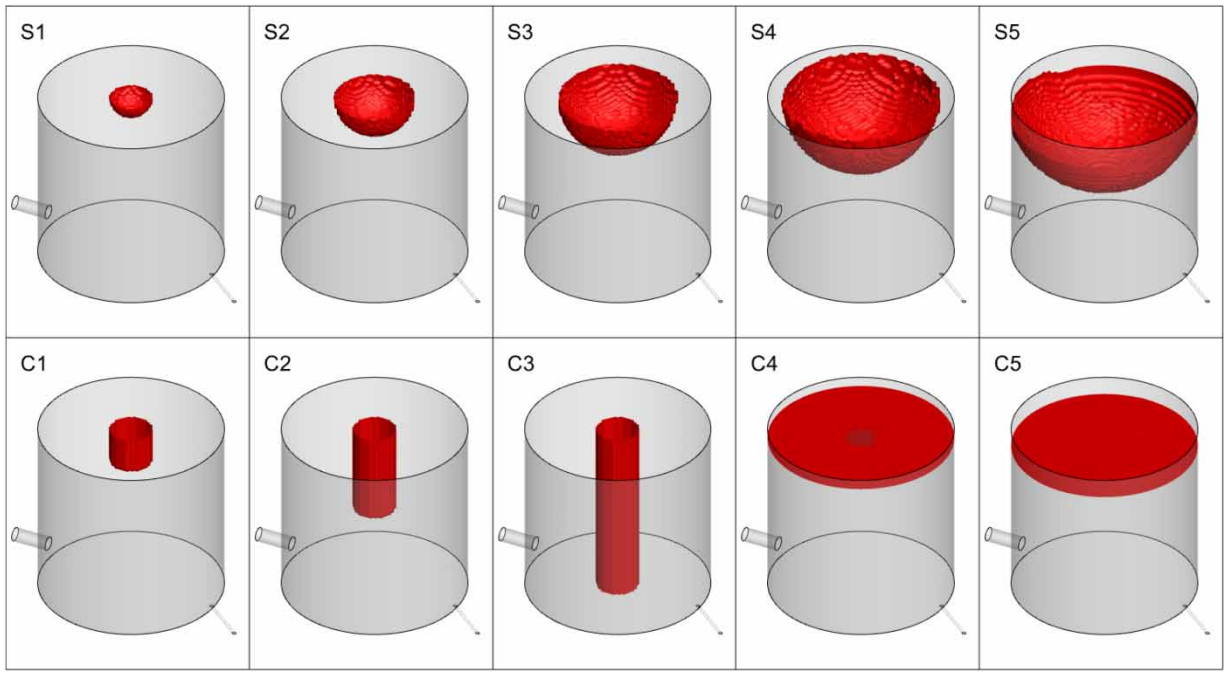

Figure 4 | Iso-surface of tracer concentration at 50% of initial concentration at the beginning of instantaneous pouring tests.

Table 1 | Description of the tracer release approaches considered in this study

	Short name of scenario	Initial spatial distribution of tracer	Description
Instantaneous Pouring	S1	Semi-sphere, radius 50 mm	Low vertical pouring momentum; Smallest pouring volume
	S2	Semi-sphere, radius 100 mm	Low vertical pouring momentum; Small pouring volume
	S3	Semi-sphere, radius 150 mm	Low vertical pouring momentum; Medium pouring volume
	S4	Semi-sphere, radius 200 mm	Low vertical pouring momentum; Large pouring volume
	S5	Semi-sphere, radius 250 mm	Low vertical pouring momentum; Largest pouring volume
	C1	Column, radius 50 mm, height 100 mm	Medium vertical pouring momentum
	C2	Column, radius 50 mm, height 250 mm	Higher vertical pouring momentum
	C3	Column, radius 50 mm, height 500 mm	Extreme high pouring momentum
	C4	Column, radius 250 mm, height 25 mm	Sprayed at surface; Low vertical pouring momentum
	C5	Column, radius 250 mm, height 50 mm	Sprayed at surface; Higher vertical pouring momentum
Quill Injecting	Q1	N/A	Quill injecting for 1 second
	Q2	N/A	Quill injecting for 4 seconds
	Q3	N/A	Quill injecting for 10 seconds

inlet to the top corner of the middle plane where the inlet and outlet are located and then most of the flow turns to the other top corner once it hits the wall and water surface. After that it goes down to the outlet, creating a symmetrical recirculation, in which the velocity is relatively slow, on each side of middle plane. By comparing the snapshots of streamline and velocity at different times (i.e., 10, 23, and 35 seconds), shown in Figure 5, it is observed that the influent jet flow is unsteady, and it is expected since it is the inherent nature of a jet flow. It is also observed that the high-speed jet from the inlet swings up and down with a cycle time of about 25 seconds.

The jet flow along with its unsteady feature serves as the main mechanism of the mixing in the tank by generating turbulence and providing energy for mixing. Therefore, for the instantaneous pouring approach, the portion of tracer that falls into the high-speed region at the beginning would be quickly mixed in the early period. Figure 6 shows the tracer distribution after tracer was released for 10 seconds. Note that, since the total amount of tracer injected into the tank varies for each different scenario, the tracer concentration in Figures 6 through 11 was normalized by the completely mixed concentration in each scenario. It is apparent that the scenarios of semi-sphere initial distribution (scenario S1 through S5) have a similar tracer distribution at this moment, while the scenario with the largest initial spread area (i.e. scenario S5) has the best mixing, as expected. High concentration can be found near the water surface in all the semi-sphere scenarios and in the region close to the outlet for those scenarios with a small initial tracer spread area.

The scenarios with the cylindrical initial tracer distributions (i.e. scenario C1 through C3) have a significantly different tracer distribution at this moment. The reason for the difference could be that some of the initial tracer distributions crossed the high-speed jet while the others did not. For example, the initial tracer in scenario C1 did not reach the high-speed jet region; the initial tracer in scenario C2 just touched the high-speed jet region; the initial tracer in scenario C3 crossed the high-speed jet region. For the same reason, the scenarios with the squat cylinder initial tracer distributions had a quite similar tracer distribution at this moment since both two scenarios had no interference from the high-speed jet. The results indicate that for the instantaneous pouring approach, less interference from the high-speed jet would reduce the difference of tracer transport.

As time advanced to 20 seconds, tracer distribution in the tank became more uniform and the differences between scenarios became less significant, as shown in Figure 7. The scenarios of S5 and C3 show the best mixing at this moment. As

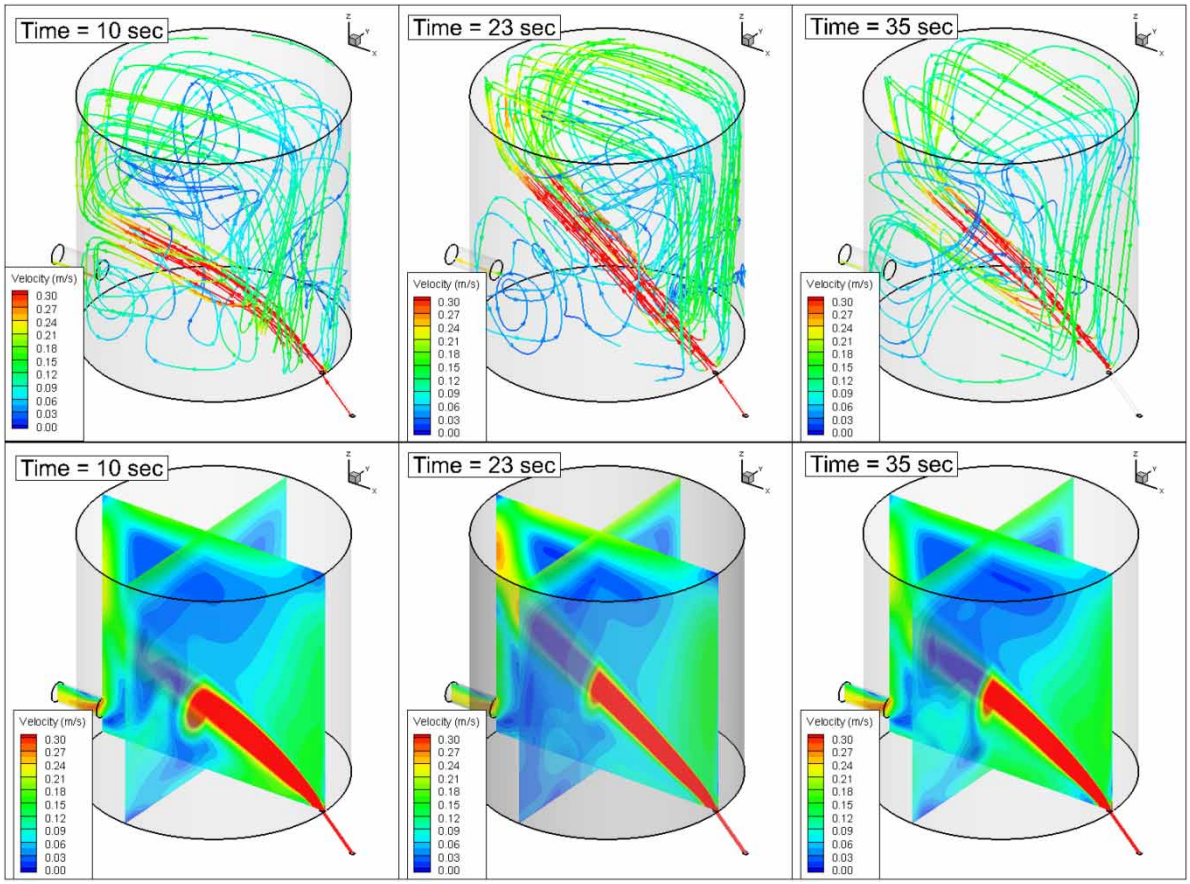

Figure 5 | Streamline and Velocity snapshots at different times (about 13 seconds' interval) showing unsteady flow. (Water flow only, no tracer considered).

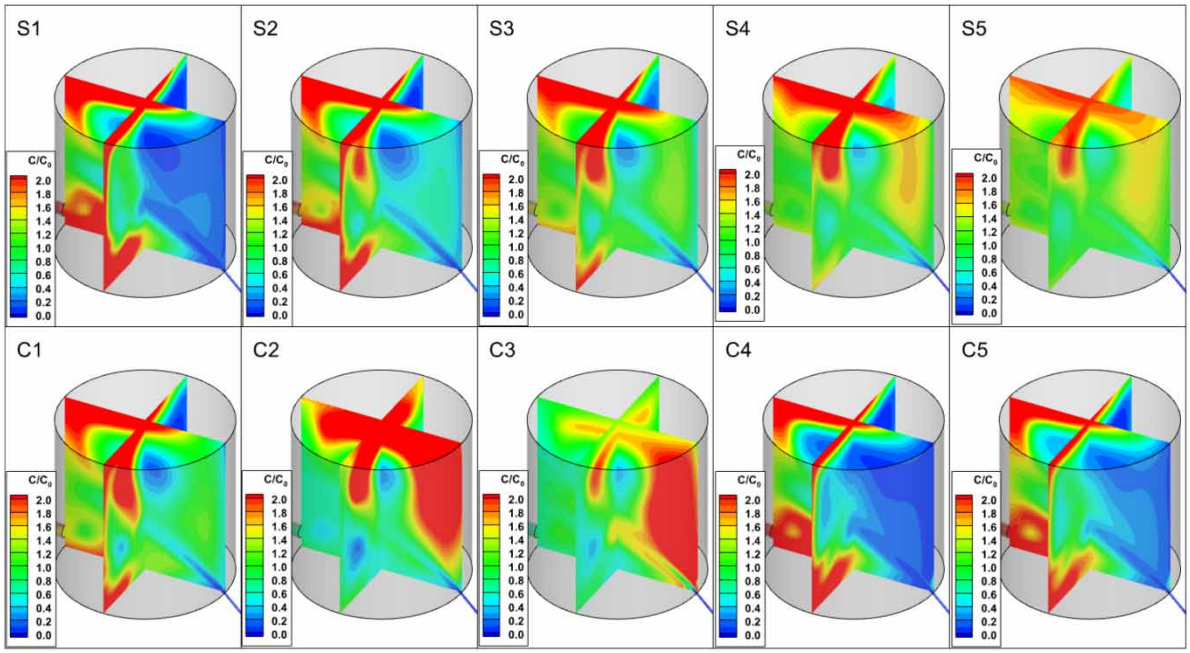

Figure 6 | Normalized tracer snapshots at time=10 seconds for the ten possible scenarios with the instantaneous pouring approach. Refer Table 1 for the description of the ten scenarios.

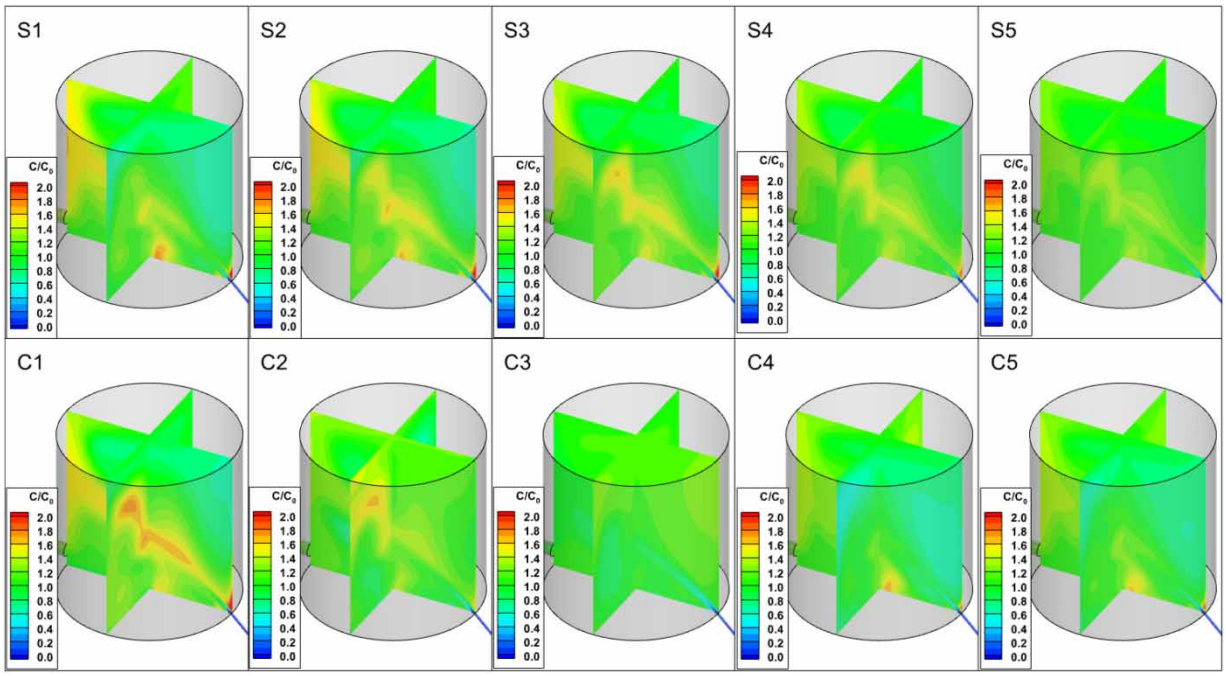

Figure 7 | Normalized tracer snapshots at time=20 seconds for the ten possible scenarios with the instantaneous pouring approach. Refer Table 1 for the description of the ten scenarios.

time advanced to 30 seconds, the tracer distribution of all scenarios became very uniform, shown in Figure 8, indicating a well-mixed state has been reached.

Figure 9 compares the tracer transport in the scenarios with a quill tracer injection. In the three scenarios, although the total amount of tracer varies depending on the release time, tracer travels roughly along a similar path as the streamlines

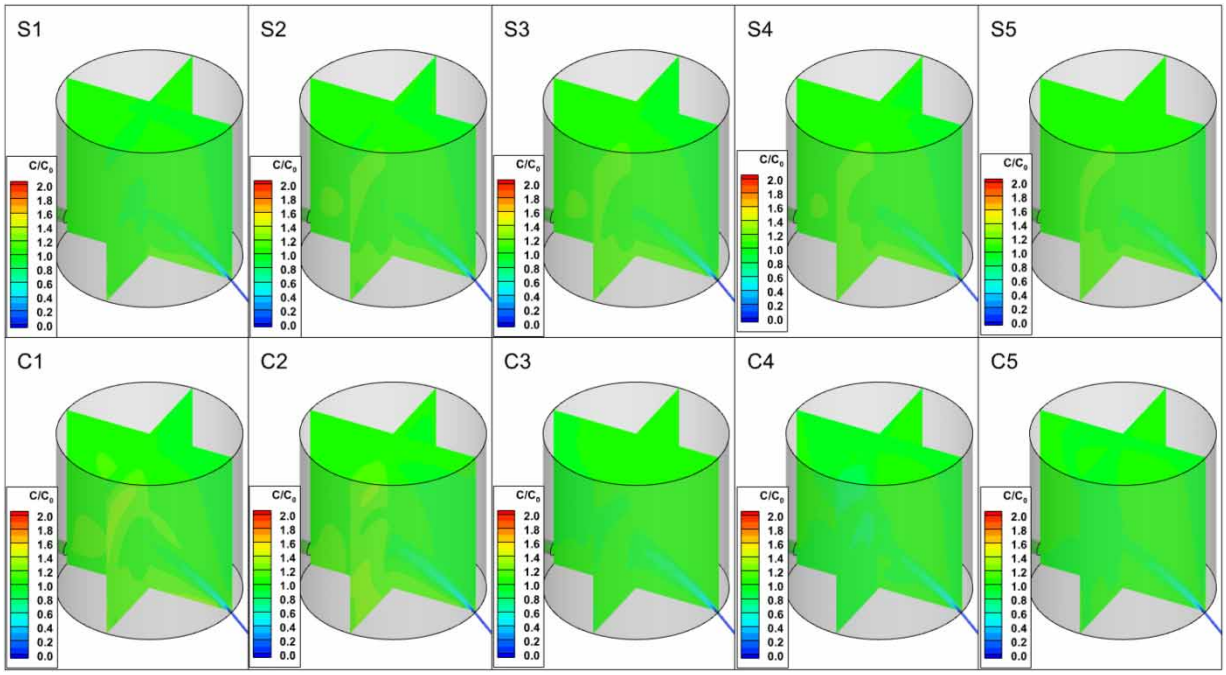

Figure 8 | Normalized tracer snapshots at time=30 seconds for the ten possible scenarios with the instantaneous pouring approach. Refer Table 1 for the description of the ten scenarios.

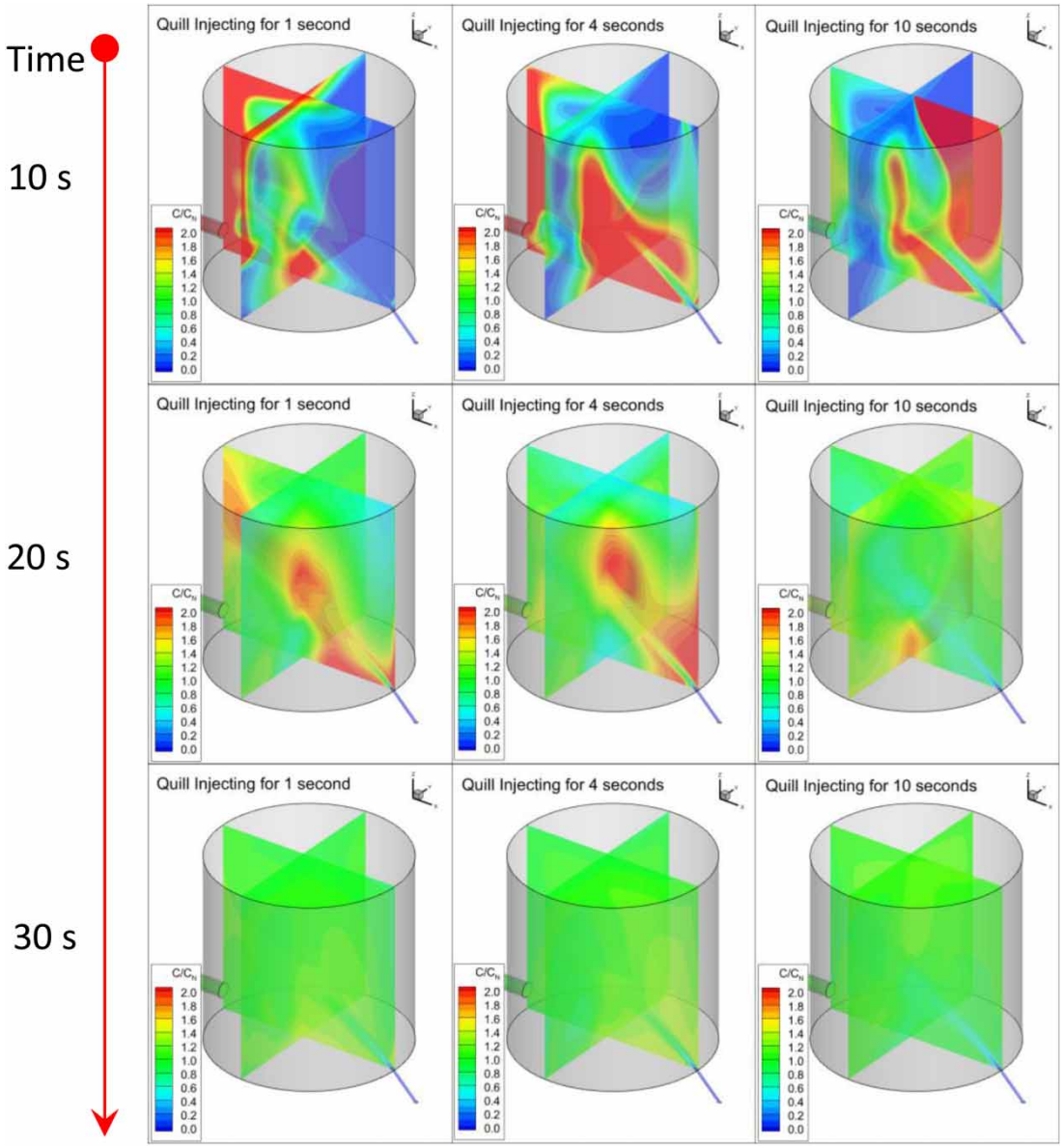

Figure 9 | Tracer snapshots at different times (i.e., 10, 20, and 30 seconds) for the three scenarios with the quill injecting approach (initial quill injecting for 1, 4, and 10 seconds respectively).

shown in Figure 5. Like the instantaneous pouring method, the tracer distribution in all the three scenarios became very uniform at 30 seconds after the tracer was initially released.

Probe tracer curve and CoV decay curve

A five-point average of CFD predicted tracer concentration near the probe sensors was calculated and compared with the data measured by probe sensors in terms of time series. Figures 10 and 11 illustrate the comparison of tracer curves at probe sensors 1 and 2, respectively.

Figure 10(a) compares the semi-sphere scenarios with the measurement at probe sensor 1. Like the measurement, the tracer curve predicted by CFD is also characterized by a breakthrough jump (a rapid increase of tracer concentration) and several peaks with the peak value decreasing over time. Overall, all tracer curves of the semi-sphere scenarios match the shape and primary peak location of the measurement well while differentiated at the breakthrough point and the primary peak value, as shown in Table 2. Among them, the tracer curve predicted in the scenario S3 has the best agreement with the measurement.

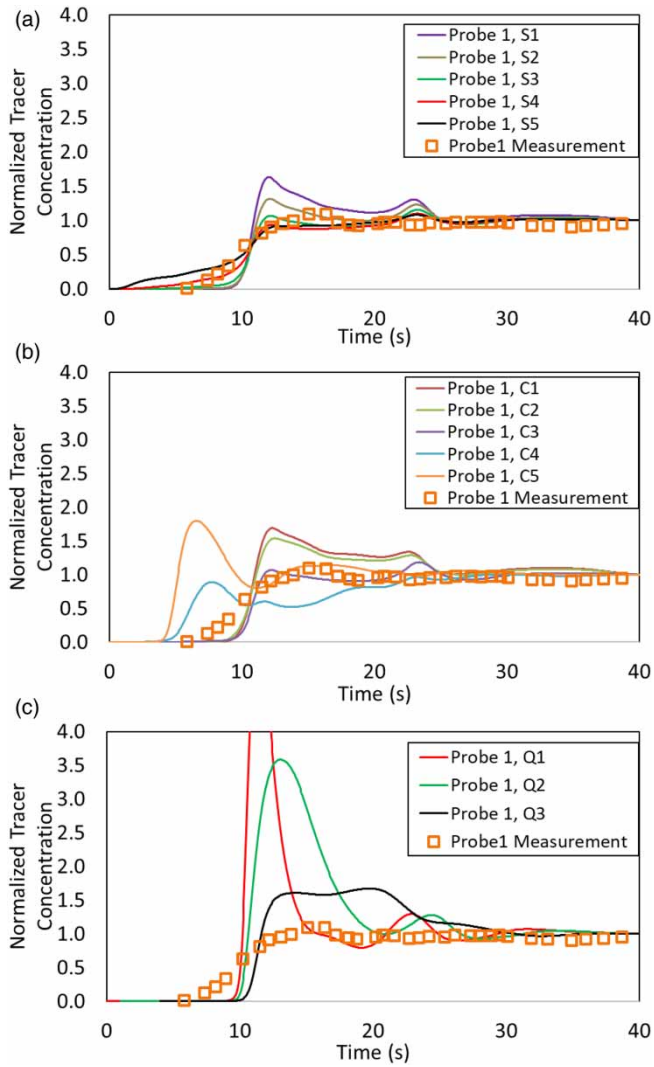

Figure 10 | Comparison of tracer curves at probe sensor 1 for (a) the semi-sphere scenarios, (b) the cylinder scenarios, and (c) the quill injecting scenarios. Refer Table 1 for the description of the scenarios.

However, all the semi-sphere scenarios predicted a quite different tracer curve at probe sensor 2, with the primary peaks being earlier and higher than the measurement (see Figure 11(a) and Table 3).

Figure 10(b) compares the cylinder scenarios with the measurement at probe sensor 1. All five scenarios have a different curve, though all of them are characterized by a breakthrough jump and primary and secondary peaks. The scenario C1 predicted a tracer curve close to the measurement except the secondary peak was slightly overestimated. However, all the scenarios poorly predict tracer curve at probe sensor 2, as all of them significantly overestimated the primary peak (see Figure 11(b) and Table 3).

Figure 10(c) compares the quill injecting scenarios with the measurement at probe sensor 1. The Q1 and Q2 scenarios predicted the primary peak location close to the measurement but significantly overestimated its value. The Q3 scenario predicted a curve with a lower peak value, but the breakthrough jump is later than the measurement. At probe sensor 2, the primary peaks predicted by the Q1 and Q2 scenarios are significantly higher than the measurement as well, as shown in Figure 11(c) and Table 3. Overall, the curves predicted in the Q3 scenario has a good agreement with the measurement at both probe sensors 1 and 2, indicating that the Q3 scenario is closest to the scenario in the physical test.

In summary, the tracer curve at a probe sensor only represents the local mixing near the probe sensor and therefore can be significantly affected by the tracer release method and the initial tracer distribution. In all the scenarios considered in this study, the predicted tracer curve may have a good agreement with the measurement at one probe while a poor agreement

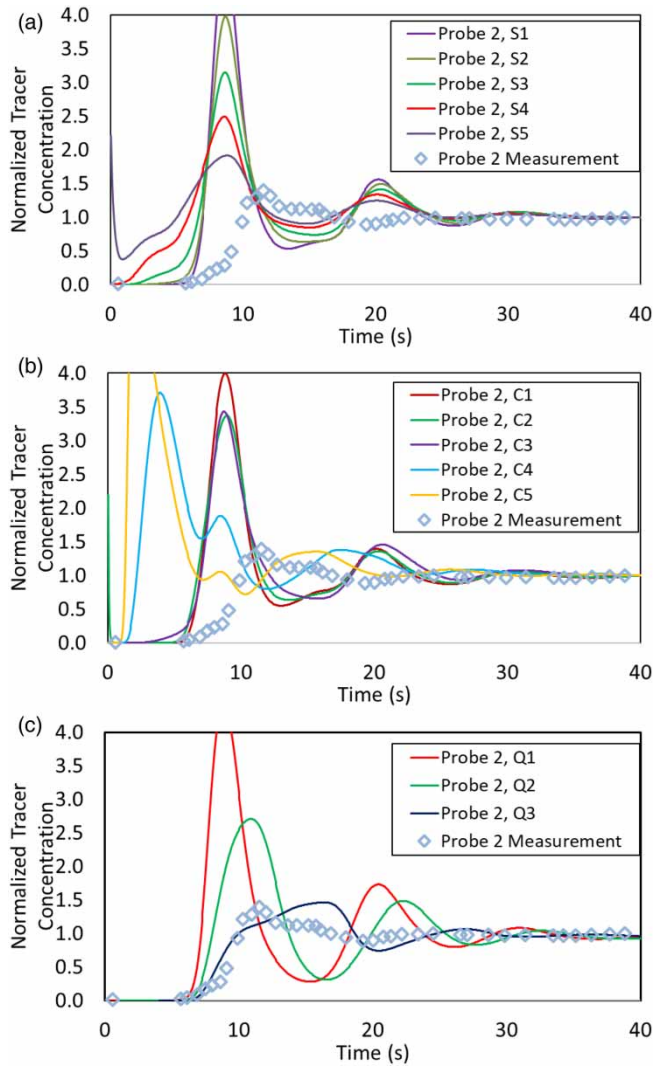

Figure 11 | Comparison of tracer curves at probe sensor 2 for (a) the semi-sphere scenarios, (b) the cylinder scenarios, and (c) the quill injecting scenarios. Refer Table 1 for the description of the scenarios.

at the other probe. It suggests that how to release the tracer is essential for a physical tracer study. The details of tracer release method should be documented.

Table 4 lists the mixing time estimated from the probe sensor tracer curves. Recall that to determine mixing time through a tracer curve, the mixing time was considered as the time it takes to reach 95% of the completely mixed concentration (Patwardhan & Gaikwad 2003). However, as observed in the CFD results and in the measurement, the tracer concentration can reach 95% of the completely mixed concentration several times since oscillations exist. This brings a difficulty in determining the mixing time in practice. In this study, the first time that the tracer concentration reaches 95% of the completely mixed concentration was considered as the mixing time. As shown in Table 4, the mixing times determined by tracer curves have a wide range (i.e., 5.1–22.1 seconds for probe 1 and 1.3–9.5 seconds for probe 2), and, in general, the mixing times determined by probe 2 tracer curves are lower than those determined by probe 1 tracer curve. This is mainly caused by the fact that the flow pattern in the tank makes probe 2 detects tracer earlier than probe 1. If estimating the mixing time from the measured data, the mixing times determined by the probes 1 and 2 are 12.0 and 9.8 seconds, respectively. The CFD predictions from the scenario Q3 are the closest to these estimated from the measured data, which is consistent with the finding from the tracer curves.

Besides estimating mixing time from a tracer curve, mixing time can be estimated from a CoV decay curve as well. Note that, it may be inconvenient to generate a CoV decay curve from a physical model since flow visualization equipment or multiple probe sensors are needed. In contrast, CFD model provides an easy-access tool to generate this CoV decay curve.

Table 2 | Locations and values of the primary peak of the tracer curves at probe sensor 1

PROBE 1	LOCATION (SECONDS)		VALUE (DIMENSIONLESS)	
Measurement	15.0	–	1.10	–
S1	12.2	−19%	1.60	45%
S2	12.4	−17%	1.30	18%
S3	12.3	−18%	1.06	−4%
S4	12.2	−19%	0.93	−15%
S5	12.0	−20%	0.90	−18%
C1	12.4	−17%	1.68	53%
C2	12.4	−17%	1.54	40%
C3	12.4	−17%	1.06	−4%
C4	7.8	−48%	0.89	−19%
C5	6.8	−55%	1.79	63%
Q1	11.4	−24%	5.60	409%
Q2	13.4	−11%	3.56	224%
Q3	14.3	−5%	1.61	46%

Refer Table 1 for the description of the scenarios.

Table 3 | Locations and values of the primary peak of the tracer curves at probe sensor 2

PROBE 2	LOCATION (SECONDS)		VALUE (DIMENSIONLESS)	
Measurement	11.5	–	1.39	–
S1	8.7	−24%	4.90	253%
S2	8.7	−24%	3.98	186%
S3	8.7	−24%	3.15	127%
S4	8.7	−24%	2.48	78%
S5	8.9	−23%	1.91	37%
C1	8.9	−23%	3.99	187%
C2	9.1	−21%	3.35	141%
C3	8.7	−24%	3.43	147%
C4	3.9	−66%	3.71	167%
C5	2.2	−81%	6.68	381%
Q1	9.0	−22%	4.40	217%
Q2	10.9	−5%	2.71	95%
Q3	11.1	−3%	1.11	−20%

Refer Table 1 for the description of the scenarios.

Figure 12 compares the CoV decay curves of all the scenarios. Although tracer release methods are different, the CoV decay curves are similar. This is consistent with the fact that the overall mixing performance of a water tank should only be related to the configuration and operation conditions and should not be affected by the tracer study method. Table 5 shows that the mixing times determined by CoV decay curves fall into a relatively small range (21.5–32.7 seconds), indicating this method is reliable and robust in determining mixing time.

Note that, the average mixing times estimated by probe tracer curves are 11.6 seconds (probe 1) and 6.3 seconds (probe 2) while that estimated by the CoV decay curve is 27.2 seconds. From the tracer distribution contour shown in Figures 6 through 9, tracer was not well mixed at 10 seconds but reached a well mixing state at 30 seconds. Therefore, the mixing time estimated by

Table 4 | Comparison of mixing times determined by probe tracer curves

Time	Mixing Time (s) Probe 1	Deviation from the Average	Mixing Time (s) Probe 2	Deviation from the Average
Measurement	12.0	4%	9.8	55%
S1	10.9	−6%	6.9	9%
S2	11.0	−5%	6.8	8%
S3	11.3	−2%	6.5	3%
S4	11.8	2%	5.6	−11%
S5	12.2	5%	4.6	−27%
C1	11.4	−1%	6.9	9%
C2	22.1	91%	2.1	−67%
C3	5.1	−56%	1.3	−79%
C4	10.9	−6%	6.8	8%
C5	11.0	−5%	6.6	5%
Q1	10.2	−12%	7.1	12%
Q2	10.6	−8%	7.9	25%
Q3	11.5	−1%	9.5	50%
Average	11.6	–	6.3	–

Refer Table 1 for the description of the scenarios.

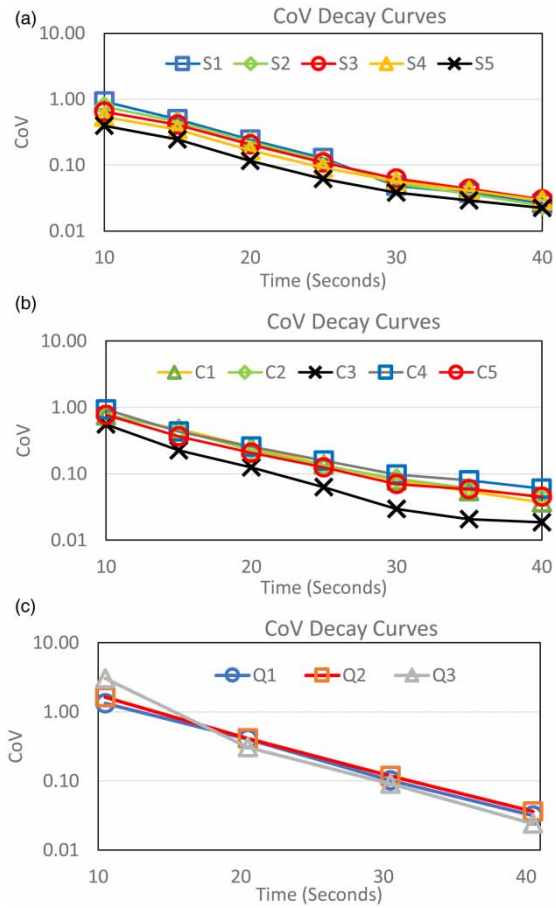

Figure 12 | CoV (Coefficient of variation) decay curves of the tracer simulation for (a) the semi-sphere scenarios, (b) the cylinder scenarios, and (c) the quill injecting scenarios. Refer Table 1 for the description of the scenarios.

Table 5 | Comparison of mixing times determined by COV (coefficient of variation) decay curves in all the scenarios considered in this study

Time	Mixing time (s)	Deviation from the average
S1	26.7	−2%
S2	26.3	−3%
S3	26.0	−4%
S4	24.4	−10%
S5	21.5	−21%
C1	28.2	4%
C2	28.4	5%
C3	22.0	−19%
C4	29.8	10%
C5	27.3	1%
Q1	30.7	13%
Q2	32.7	20%
Q3	29.0	7%
Average	27.2	–

Refer Table 1 for the description of the scenarios.

the CoV decay curve is more accurate and conservative. It indicates that the mixing time determined by the probe sensor tracer curve cannot serve as a proper index for the global mixing in a water storage tank, while the mixing time determined by a CoV decay curve is a more appropriate index. It suggests that the mixing time in a water tank should be determined by a CoV decay curve in future mixing performance studies no matter whether they involve a physical experiment or a CFD simulation.

CONCLUSION

This study compared the tracer curves at probe sensor locations from scenarios with different tracer introducing approaches and found that the tracer curve measured by a probe sensor: (1) is sensitive to the tracer introducing approach. The probe tracer curve can vary significantly even when the overall mixing performance is similar. This could be a potential explanation for the discrepancy between the CFD prediction and physical measurement in Marek *et al.* (2007); (2) also varies significantly at different locations; (3) has oscillations, bringing in difficulty and uncertainty in determining mixing time. Therefore, the probe tracer curve can only represent local mixing, while it is not an appropriate way to evaluate overall mixing in a storage tank.

For the same scenarios, this study also compared the CoV decay curves. It was found that tracer introducing approaches have a minor impact on the CoV decay curve. Consequently, the mixing time estimated by the CoV decay curve is relatively consistent (deviates from −21% to +20%) compared to those determined by the probe tracer curves (deviates from −79% to 91%).

Besides, from the observed tracer distribution, the tracer mixed well at the average mixing time estimated by the CoV decay curve, while it did not at the average mixing time estimated by the probe tracer curve. This indicates that the mixing time estimated by the CoV decay curve is more accurate and conservative.

In summary, it is more appropriate to determine the mixing time in a water storage tank through a CoV decay curve rather than a probe tracer curve, no matter whether using a physical test or a CFD simulation. In further physical tracer studies for evaluating mixing performance in a water storage tank, it is suggested that multiple sensors or other devices that can monitor tracer concentration change over time should be used to capture global mixing rather than local mixing.

Note that in this study the CFD simulations were conducted by following a physical test without knowing the details of how the tracer was released. For future study, physical tracer studies with different tracer release approaches and initial conditions should be conducted. In these physical tracer studies, besides monitoring probe tracer curve and CoV decay curve, tracer mixing over time should be visualized through a flow visualization approach to further compare the accuracy and reliability of mixing times predicted by the probe tracer curve and CoV decay curve.

DATA AVAILABILITY STATEMENT

All relevant data are included in the paper or its Supplementary Information.

REFERENCES

ANSYS Fluent 2016 *ANSYS Fluent 12.0 user's guide*. Available from: http://www.afs.enea.it/project/neptunius/docs/fluent/html/ug/main_pre.htm (accessed 29 July 2020).

Bumrungthaichaichan, E. 2016 A review on numerical consideration for computational fluid dynamics modeling of jet mixing tanks. *Korean Journal of Chemical Engineering* **33** (11), 3050–3068.

Gaikwad, S. G. 2001 *Studies in Jet Mixed Tanks*, Master Thesis, University of Mumbai, Mumbai, India.

Grenville, R. K. & Tilton, J. N. 1996 A new theory improves the correlation of blend time data from turbulent jet mixed vessels. *Chemical Engineering Research & Design* **74** (3), 390–396.

Grenville, R. & Tilton, J. N. 1997 Turbulence for flow as a predictor of blend time in turbulent jet mixed vessels. In: *Proceedings of the Nineth European Conference on Mixing*, March, pp. 67–74.

Grenville, R. K. & Tilton, J. N. 2011 Jet mixing in tall tanks: comparison of methods for predicting blend times. *Chemical Engineering Research and Design* **89** (12), 2501–2506.

Hurtig, K. I. 2004 *Hydraulic Modelling of Water Treatment Storage Tanks for Disinfection Contact Time*. Master Thesis, University of Alberta, Canada.

Launder, B. E. 1978 Heat and mass transport (Chap. 6). In: *Turbulence* (Bradshaw, P., ed.). Springer, Berlin.

Marek, M., Stoesser, T., Roberts, P. J., Weitbrecht, V. & Jirka, G. H. 2007 CFD modeling of turbulent jet mixing in a water storage tank. In: *Proceedings of the Congress-International Association for Hydraulic Research*. Vol. 32, No. 2, p. 551.

Orfaniotis, A., Fonade, C., Lalane, M. & Doubrovine, N. 1996 Experimental study of the fluidic mixing in a cylindrical reactor. *The Canadian Journal of Chemical Engineering* **74** (2), 203–212.

Patwardhan, A. W. & Gaikwad, S. G. 2003 Mixing in tanks agitated by jets. *Chemical Engineering Research and Design* **81** (2), 211–220.

Roberts, P. J. W. 2006 *Physical Modeling of Mixing in Water Storage Tanks*. American Water Works Association. Denver, CO, United States.

Rossman, L. A. & Grayman, W. M. 1999 Scale-model studies of mixing in drinking water storage tanks. *Journal of Environmental Engineering* **125** (8), 755–761.

Sautner, J. B., Maslia, M. L. & Grayman, W. M. 2007 Storage tank mixing models: comparison of tracer data with model simulation. In: *World Environmental and Water Resources Congress 2007: Restoring Our Natural Habitat*, pp. 1–11.

Simon, M. & Fonade, C. 1993 Experimental study of mixing performances using steady and unsteady jets. *The Canadian Journal of Chemical Engineering* **71** (4), 507–513.

Tian, X. & Roberts, P. J. 2008a Mixing in water storage tanks. I: no buoyancy effects. *Journal of Environmental Engineering* **134** (12), 974–985.

Tian, X. & Roberts, P. J. 2008b Mixing in water storage tanks. II: with buoyancy effects. *Journal of Environmental Engineering* **134** (12), 986–995.

Wilcox, D. C. 1994 *Turbulence Modeling for CFD*. DCW Industries, La Cañada Flintridge, CA.

Xavier, M. L. M. & Janzen, J. G. 2017 Effects of inlet momentum and orientation on the hydraulic performance of water storage tanks. *Applied Water Science* **7** (5), 2545–2557.

Zhang, J., Pierre, K. C. & Tejada-Martinez, A. E. 2019a Impacts of flow and tracer release unsteadiness on tracer analysis of water and wastewater treatment facilities. *Journal of Hydraulic Engineering* **145** (4), 04019004.

Zhang, J., Xu, X., Tejada-Martinez, A., Zhang, Q. & Wicklein, E. 2019b Evaluating reactor hydraulics in a cost-effective and environment-friendly way: numerical tracer study. *AWWA Water Science* **1** (6), e1163.

First received 16 July 2021; accepted in revised form 28 December 2021. Available online 19 January 2022